

RESEARCH ARTICLE

Interpretable machine learning-based individual analysis of acute kidney injury in immune checkpoint inhibitor therapy

Minoru Sakuragi^{1,2}, Eiichiro Uchino^{1,2}, Noriaki Sato^{1,2}, Takeshi Matsubara², Akihiko Ueda^{1,3}, Yohei Mineharu^{1,4,5}, Ryosuke Kojima¹, Motoko Yanagita^{2,6*}, Yasushi Okuno^{1*}

1 Department of Biomedical Data Intelligence, Graduate School of Medicine, Kyoto University, Kyoto, Japan, **2** Department of Nephrology, Graduate School of Medicine, Kyoto University, Kyoto, Japan, **3** Department of Gynecology and Obstetrics, Graduate School of Medicine, Kyoto University, Kyoto, Japan, **4** Department of Neurosurgery, Graduate School of Medicine, Kyoto University, Kyoto, Japan, **5** Department of Artificial Intelligence in Healthcare and Medicine, Graduate School of Medicine, Kyoto University, Kyoto, Japan, **6** Institute for the Advanced Study of Human Biology (ASHBi), Kyoto University, Kyoto, Japan

* okuno.yasushi.4c@kyoto-u.ac.jp (YO); motoy@kuhp.kyoto-u.ac.jp (MY)



OPEN ACCESS

Citation: Sakuragi M, Uchino E, Sato N, Matsubara T, Ueda A, Mineharu Y, et al. (2024) Interpretable machine learning-based individual analysis of acute kidney injury in immune checkpoint inhibitor therapy. PLoS ONE 19(3): e0298673. <https://doi.org/10.1371/journal.pone.0298673>

Editor: Giuseppe Remuzzi, Istituto Di Ricerche Farmacologiche Mario Negri, ITALY

Received: September 14, 2023

Accepted: January 30, 2024

Published: March 19, 2024

Peer Review History: PLOS recognizes the benefits of transparency in the peer review process; therefore, we enable the publication of all of the content of peer review and author responses alongside final, published articles. The editorial history of this article is available here: <https://doi.org/10.1371/journal.pone.0298673>

Copyright: © 2024 Sakuragi et al. This is an open access article distributed under the terms of the [Creative Commons Attribution License](https://creativecommons.org/licenses/by/4.0/), which permits unrestricted use, distribution, and reproduction in any medium, provided the original author and source are credited.

Data Availability Statement: Data cannot be shared publicly because of patient privacy in electronic medical records. Data are available from Kyoto University Graduate School and Faculty of

Abstract

Background

Acute kidney injury (AKI) is a critical complication of immune checkpoint inhibitor therapy. Since the etiology of AKI in patients undergoing cancer therapy varies, clarifying underlying causes in individual cases is critical for optimal cancer treatment. Although it is essential to individually analyze immune checkpoint inhibitor-treated patients for underlying pathologies for each AKI episode, these analyses have not been realized. Herein, we aimed to individually clarify the underlying causes of AKI in immune checkpoint inhibitor-treated patients using a new clustering approach with Shapley Additive exPlanations (SHAP).

Methods

We developed a gradient-boosting decision tree-based machine learning model continuously predicting AKI within 7 days, using the medical records of 616 immune checkpoint inhibitor-treated patients. The temporal changes in individual predictive reasoning in AKI prediction models represented the key features contributing to each AKI prediction and clustered AKI patients based on the features with high predictive contribution quantified in time series by SHAP. We searched for common clinical backgrounds of AKI patients in each cluster, compared with annotation by three nephrologists.

Results

One hundred and twelve patients (18.2%) had at least one AKI episode. They were clustered per the key feature, and their SHAP value patterns, and the nephrologists assessed the clusters' clinical relevance. Receiver operating characteristic analysis revealed that the area under the curve was 0.880. Patients with AKI were categorized into four clusters with significant prognostic differences ($p = 0.010$). The leading causes of AKI for each cluster,

Medicine, Ethics Committee via email (ethcom@kuhp.kyoto-u.ac.jp) or telephone (+81-75-753-4680) for researchers who meet the criteria for access to confidential data.

Funding: The authors received no specific funding for this work.

Competing interests: The authors have declared that no competing interests exist.

such as hypovolemia, drug-related, and cancer cachexia, were all clinically interpretable, which conventional approaches cannot obtain.

Conclusion

Our results suggest that the clustering method of individual predictive reasoning in machine learning models can be applied to infer clinically critical factors for developing each episode of AKI among patients with multiple AKI risk factors, such as immune checkpoint inhibitor-treated patients.

Introduction

Acute kidney injury (AKI) is a critical complication with significant prognostic implications often observed in cancer patients [1–3]. Immune checkpoint inhibitors (ICIs) are key therapeutic agents for advanced cancer that can cause renal-related adverse events during their administration, including AKI [4–8]. With the increasing use of ICIs, the incidence of AKI during ICI therapy has been reported to be as high as 14–18% [9–11]. The development of AKI during systemic therapy, such as ICI therapy, not only increases the risk of death and the adverse effects on multiple organs but also represents a major cause of interruption of cancer treatment [1, 2]. Several risk factors for AKI, including baseline renal function, proton pump inhibitors (PPI), and immune-related adverse events (IrAEs), have been reported in ICI-treated patients [12–17]. However, these studies analyzed the population as a whole and did not perform individual risk analyses for each AKI episode in each patient. Since the etiology of AKI in patients undergoing cancer therapy varies, even among those diagnosed with the same type of AKI, clarifying the causes of AKI is critical for achieving optimal cancer treatment. Therefore, it is essential to individually analyze ICI-treated patients for existing underlying pathologies causing the onset of each episode of AKI. However, these individual analyses have not yet been realized with conventional clinical research methods, and no such study has been reported.

Herein, we investigated the underlying background of AKI in ICI-treated patients by applying a new approach to classify and analyze time-series individual predictive reasoning of machine learning (ML)-based AKI prediction models. First, we focused on the fact that the temporal changes in individual predictive reasoning in continuous AKI prediction models represent the key features contributing to each AKI prediction. We then estimated that in AKI prediction models, patients with similar predictive reasoning shared similar underlying factors for AKI development, and clustered AKI patients based on the pattern of features with high predictive contribution quantified in time-series by SHapley Additive exPlanations (SHAP) [18]. Thus, we compared each cluster with nephrologist chart review findings, which revealed crucial underlying factors involved in AKI development in individual ICI-treated patients that were not previously observed. Furthermore, the predictive reasoning consisted of combinations of features reasonably interpretable by clinicians.

Our results enabled us to clarify the background of AKI development in ICI-treated patients with underlying risks for AKI and suggested the potential for medical applications of ML prediction models as interpretable artificial intelligence (AI) to medical care, which had been a challenge to explainability.

Materials and methods

Model development and definitions

We created a dataset from the electronic medical records (EMRs) of 616 patients who received ICI therapy for cancer at the Kyoto University Hospital from July 2014 to September 2019 and constructed an AKI prediction model. Using this dataset, we constructed an ML-based model to continuously predict the development of AKI within 7 days of the reference date (S1 and S2 Figs in [S1 File](#)). Subsequently, we visualized the predictive reasoning among patients with AKI using SHAP and evaluated the clinical validity of patient clustering using predictive reasoning for AKI development ([Fig 1](#)). AKI was defined based on serum creatinine (SCr) changes (≥ 0.3 mg/dL or 1.5 times increase from baseline) according to Kidney Disease: Improving Global Outcomes diagnostic criteria [19] (S1 Method in [S1 File](#)). The period for the prediction model was defined as the period from the ICI initiation in each patient to the end of December 2019; patients with multiple AKI events within 14 days from the date of the first episode of AKI were excluded from the evaluation.

We used LightGBM [20], a gradient-boosting decision tree, as a prediction algorithm to build a classification model that would continuously predict AKI within 7 days from each time point ([Fig 1](#)). The main reasons for selecting LightGBM were its flexibility in handling medical records that potentially contain a certain number of missing values and its ability to perform high-speed calculations (S1 Table in [S1 File](#)). We used 287 clinical variables obtained from EMRs as input features for each patient (S2 Method in [S1 File](#)). For the features linked to time series, data from the 4 weeks before the reference date were divided into four windows, one for each week, and each window was labeled “(-1 wk),” “(-2 wk),” “(-3 wk),” and “(-4 wk),” and suffixes were assigned to each feature (S1 Fig in [S1 File](#)). In addition, the objective variable was labeled “AKI-positive” if the patient developed AKI within 7 days of the predicted time point (S2 Fig in [S1 File](#)). All analyses were conducted using Python 3.7.7 (<https://www.python.org/doc/>), with scikit-learn [21] 0.22.1 (<https://scikit-learn.org/stable/index.html#>) and LightGBM 2.3.0 (<https://lightgbm.readthedocs.io/en/stable/#>) libraries for model development, and statsmodels 0.13.2, rpy2 3.5.2, and lifelines 0.25.9 libraries for statistical analysis.

Visualizing individual AKI predictive reasoning and clustering

SHAP is a game theory-based model interpretation framework that quantitatively evaluates the contribution of each input feature as a SHAP value [18]. Unlike previous studies, we performed a unique visualization in which SHAP values at all prediction time points were arranged in a time series ([Fig 1](#)). The SHAP method was implemented using the Python SHAP package (<https://shap.readthedocs.io/en/latest/>).

We performed hierarchical clustering for patients with AKI based on the patterns of SHAP values and searched for common clinical backgrounds in each cluster. Subsequently, we compared the clinical backgrounds in each cluster with AKI causes, as annotated by three nephrologists (S3 Fig in [S1 File](#)). All chart reviews and the free-text annotations of the nephrologists for AKI causes were conducted independent of ML model analysis and without being influenced by each other (S3 Method in [S1 File](#)). Furthermore, we evaluated the clinical validity of the clustering by observing the 90-day survival after the first episode of AKI with the Kaplan—Meier analysis. In addition, categorical variables and means among clusters were compared using Fisher’s exact probability and Kruskal—Wallis tests, respectively. Finally, the distribution of annotation labels within each cluster was evaluated using Chi-square goodness-of-fit test. Statistical significance was defined as $p < 0.05$.

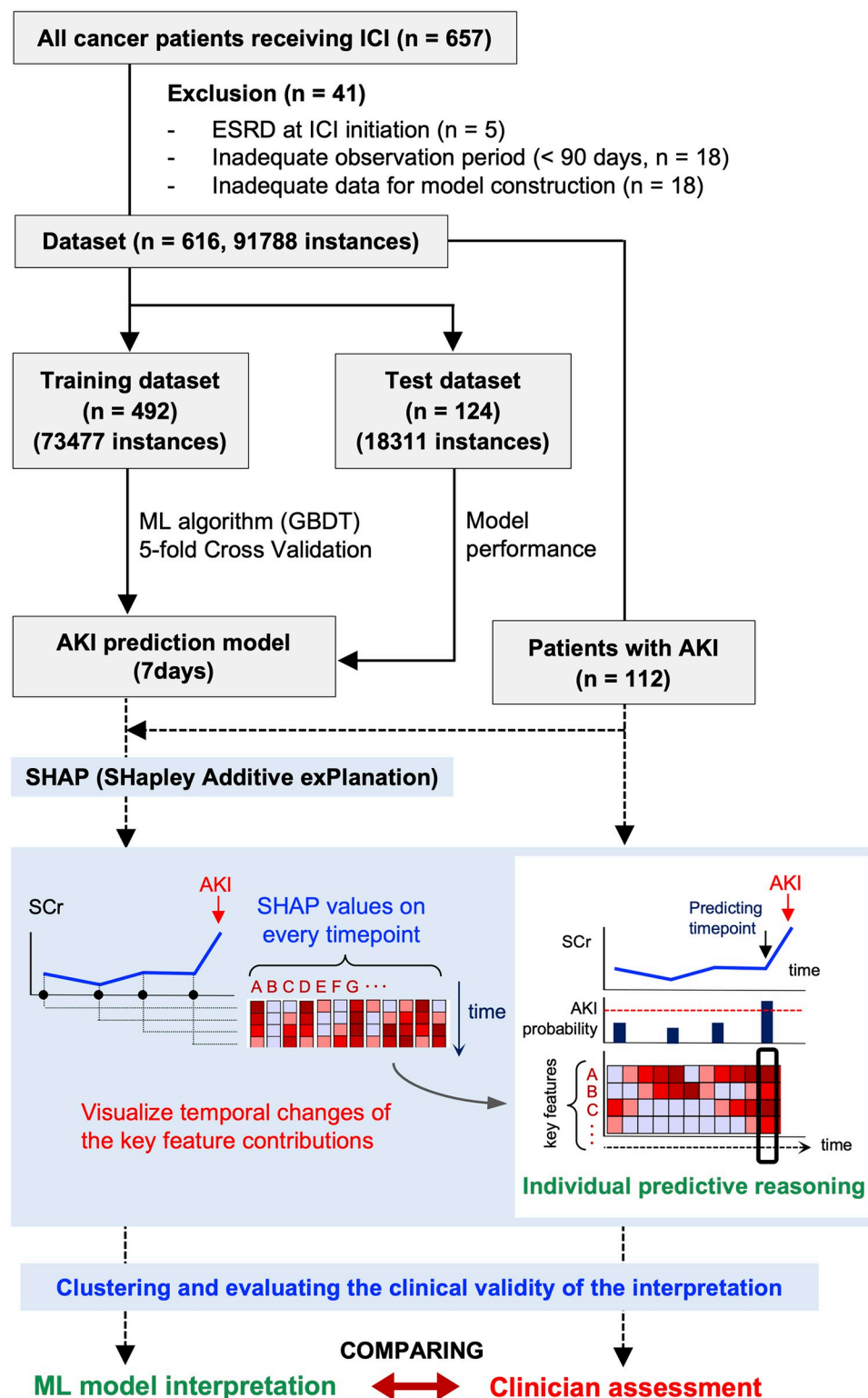


Fig 1. Analysis overview. Among the 657 ICI-treated patients, those who had end-stage renal disease (ESRD) before ICI initiation and those with missing data or inadequate periods for model construction were excluded from this study. The entire dataset was split into test (20%) and training datasets on a per-patient basis, and hyperparameter tuning of the model was performed on the training dataset (5-fold cross-validation). The contribution of key features to AKI development at each prediction time point was quantified based on SHAP values and visualized using the

heatmap. The SHAP value of each feature takes a positive or negative value as a vector of contributions, with the magnitude of the absolute value representing the degree of influence on the prediction outcome. The trend of SHAP values at the time point when the model predicts AKI (bold black box) indicates the combination of key features and their contributions (individual predictive reasoning) crucial for predicting AKI in that patient. AKI, acute kidney injury; ICI, immune checkpoint inhibitors; ESRD, end-stage renal disease; ML, machine learning; GBDT, Gradient Boosting Decision Tree; SHAP, SHapley Additive exPlanations; SCr, serum creatinine.

<https://doi.org/10.1371/journal.pone.0298673.g001>

Ethical statement and informed consent

The dataset was generated and reviewed based on the clinical information obtained from the EMR of our institution. This study was conducted using data obtained only during medical practice, according to the principles of the Declaration of Helsinki. Per Japanese laws and regulations, informed consent was obtained on an opt-out basis. All explanations of the study and expressions of consent were assured to be conducted in a written format, guaranteeing that participants received comprehensive information and their consent or dissent was appropriately recorded. This method aligns with the approval granted by the Ethical Review Board of Kyoto University, acknowledging it as a valid form of consent for this type of research. We ensured ethical compliance by publicly providing detailed information about the study, including its purpose, the nature of the data used, and the rights of participants to withdraw, on the Kyoto University Hospital website (<https://www.kuhp.kyoto-u.ac.jp/outline/research-disclosure.html>). The option for participants was made clear and accessible, thus preserving their autonomy. The Ethical Review Board of Kyoto University approved the study (Approval Number R1498), recognizing its adequacy for the nature of this retrospective analysis. The period of data access and analysis for this study was from March 2022 to August 2022. In collecting the data, the authors did not access any data that could identify individual participants.

Results

Model performance and visualizing individual predictive reasoning

Among the 616 patients, 112 (18.2%) had at least one AKI episode after initiation of ICI therapy. The clinical characteristics of the patients are presented in Table 1. The generalization performance of the model estimated based on the test data had an area under the receiver operating characteristic curve of 0.880, similar to that of the pre-existing models [22–29] (Fig 2a). Performance comparisons with other ML models are summarized in S1 Table in S1 File. The SHAP values of the key features that contributed to the prediction of AKI are presented in Fig 2b and 2c. Two examples of predictive reasoning in patients with AKI are presented in Fig 2d. Considering that the contributing factors of AKI vary across patients (Fig 2e), individual differences in predictive reasoning may reflect individual differences in clinical backgrounds related to the development of AKI.

Clustering patients with AKI using predictive reasoning

A total of 112 patients with AKI were categorized into four clusters based on predictive reasoning immediately before the first episode of AKI using unsupervised clustering (Fig 3a, Table 2), compared with annotation independently reviewed by the three nephrologists [24]. The number of clusters was determined as the number of visually valid clusters indicated on the dendrogram produced by the hierarchical clustering. Based on their descriptions, the strongest contributive risk factors for AKI development were assigned six labels for each patient: “Hypovolemia,” “Cancer Cachexia,” “Infection,” “Drug-related,” “Obstruction,” and “Others.” (S3 Method in S1 File). The number of these labels was counted in each cluster to

Table 1. Baseline characteristics of patients undergoing immune checkpoint inhibitor therapy.

	All patients (n = 616)			p-value
		With AKI (n = 112)	Without AKI (n = 504)	
Age [n (%)]				
20–39 years	17 (3)	3 (3)	14 (3)	0.954
40–59 years	107 (17)	21 (19)	86 (17)	0.773
60–79 years	415 (67)	80 (71)	335 (66)	0.367
> 80 years	77 (13)	8 (7)	69 (14)	0.082
Male [n] / Female [n]	415 / 201	82 / 30	333 / 171	0.178
Malignancy types [n (%)]				
Gastrointestinal	74 (12)	10 (9)	64 (13)	0.342
Lung	333 (54)	45 (40)	288 (57)	0.001 *
Urologic	72 (12)	23 (21)	49 (10)	0.002 *
Skin	78 (13)	28 (25)	50 (10)	< 0.001 *
Other	59 (9)	6 (5)	53 (11)	0.133
ICI types [n (%)]				
PD-1 antibody	559 (91)	103 (92)	453 (90)	0.620
PD-L1 antibody	75 (12)	11 (10)	64 (13)	0.495
CTLA-4 antibody	43 (7)	12 (11)	31 (6)	0.131
Combination therapy	22 (4)	4 (4)	18 (4)	1.000
Baseline SCr [mg/dL, median (IQR)]	0.79 (0.66–0.95)	0.90 (0.67–1.11)	0.82 (0.66–0.92)	< 0.001 *
PPI administration [n (%)]	152 (25)	33 (29)	119 (24)	0.239
NSAID administration [n (%)]	66 (11)	12 (11)	54 (11)	1.000

All data are presented as medians (interquartile range, IQR) or means (standard deviation, SD), as appropriate for nonparametric or parametric variables, respectively. Patients with ESRD at the initiation of ICI (n = 5), patients without data on renal function after ICI (n = 18), and patients whose follow-up was censored < 3 months after initiation of ICI (n = 18) were excluded from the analysis. ICIs included anti-PD-1, anti-PD-L1, and anti-CTLA-4 antibodies, while some patients received combination therapy with anti-PD-1 and anti-CTLA-4 antibodies. Comparisons of categorical variables were made using the Chi-square test or Fisher's exact probability test. ICI, immune checkpoint inhibitors; AKI, acute kidney injury; PD-1, Programmed cell death 1; PD-L1, Programmed death-ligand 1; CTLA-4, Cytotoxic T-lymphocyte-associated antigen; SCr, serum creatinine; PPI, proton pump inhibitors; NSAIDs, nonsteroidal anti-inflammatory drugs; ESRD, end-stage renal disease; IQR, interquartile range; SD, standard deviation.

<https://doi.org/10.1371/journal.pone.0298673.t001>

determine the most dominant contributive risk factor. Although the proportions of each label did not differ significantly among the clusters, each cluster had distinct patterns of contributing risk factors for the development of AKI (Fig 3b). While there was a clear trend in the label distribution within each cluster, only clusters 3 and 4 showed statistically significant differences. The most dominant labels in each cluster were as follows: cluster 1, “Hypovolemia”; cluster 2, “Drug-related”; cluster 3, “Drug-related”; and cluster 4, “Cancer Cachexia.” In addition, clusters 2 and 3 were annotated as “Drug-related,” including IrAE, while each cluster indicated different patient backgrounds (S2 Table in S1 File). These results suggested that patients categorized by predictive reasoning likely have different clinical backgrounds regarding AKI development between the clusters.

To further elucidate patient clustering by SHAP, we constructed a two-dimensional plot (dependence plot), which represents the correlation between the feature values and their SHAP values in the week before AKI development among 112 patients with AKI (Fig 3c). For example, cluster 4, which was characterized by high SHAP values for C-reactive protein (CRP) and lactate dehydrogenase (LDH), dietary intake, and diuretic use, demonstrated high CRP and LDH levels and poor dietary intake, including diuretic use in one out of three cases, which strongly contributed to AKI prediction (Fig 3a). Generally, high CRP and LDH levels and

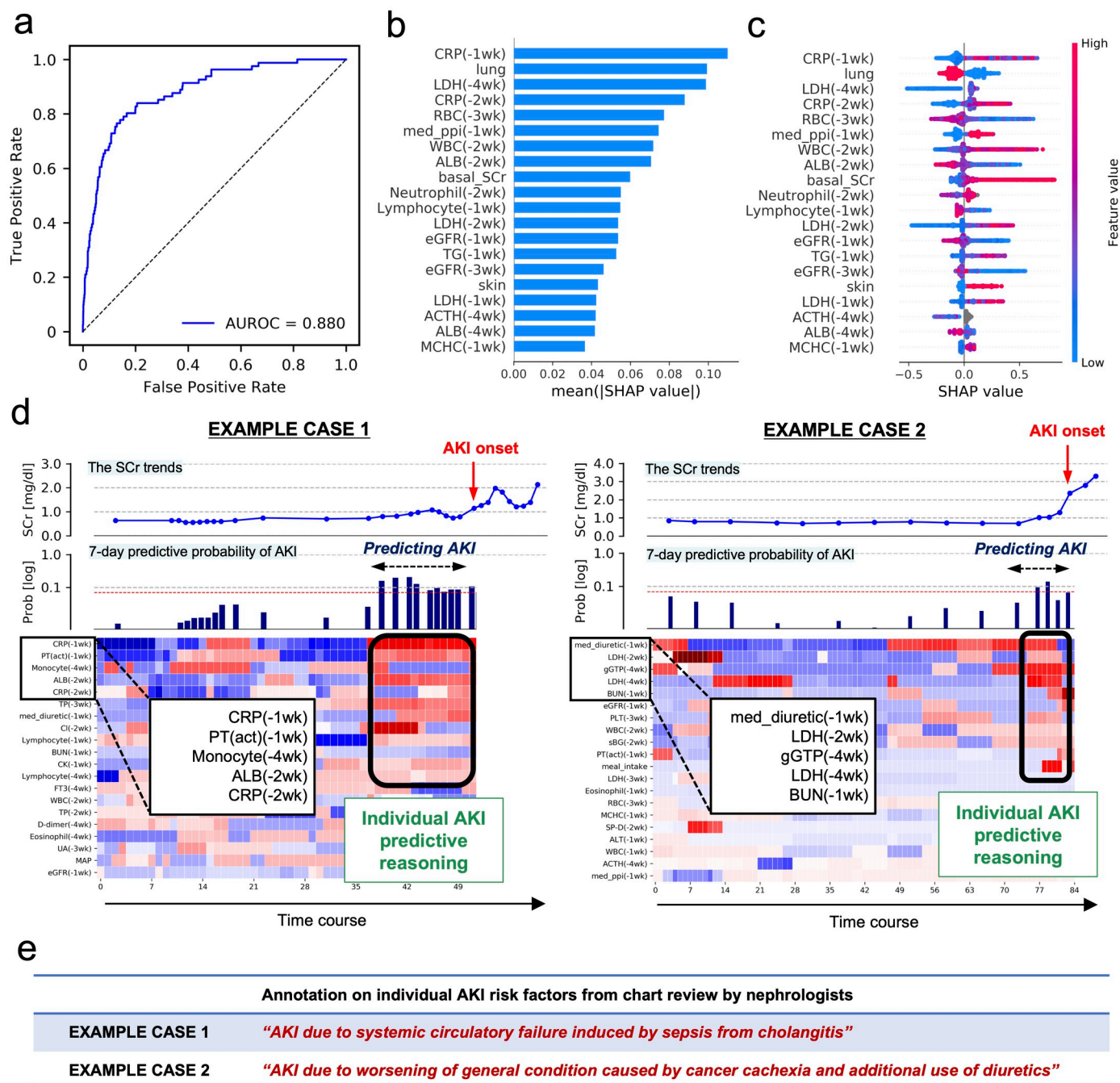


Fig 2. Model performance and visualizing individual predictive reasoning. (a) Performance of the model. The general performance is evaluated based on the area under the ROC curve. (b, c) Features indicating higher overall SHAP. Features with higher average contributions for all patients are shown. Positive and negative contributions to predicted AKI development are characterized by positive and negative SHAP values, respectively, with red and blue representing the magnitude of respective feature values. (d) Examples of individual predictive reasoning. The graph of SCr value-predicted probabilities of AKI development within 7 days, and the heatmap of SHAP values for the key features are represented on the same timeline. The red dotted line indicates the threshold value for 0.25 in the precision probabilities, and the predicted probabilities above the line are regarded as positive predictions (S5 Fig in S1 File). The bold black-boxed area, at time points with elevated predictive probability, represents the key features and their contribution to the prediction of AKI for that individual. These two examples demonstrate different heatmap patterns of SHAP, suggesting the difference in predictive reasoning. (e) Examples of nephrologists' chart reviews. The annotations of nephrologists for contributing factors to AKI development for the two cases with predictive reasoning are shown above. ROC, receiver operating characteristic curve; SHAP, SHapley Additive exPlanations; AKI, acute kidney injury; SCr, serum creatinine; IrAEs, immune-related adverse events.

<https://doi.org/10.1371/journal.pone.0298673.g002>

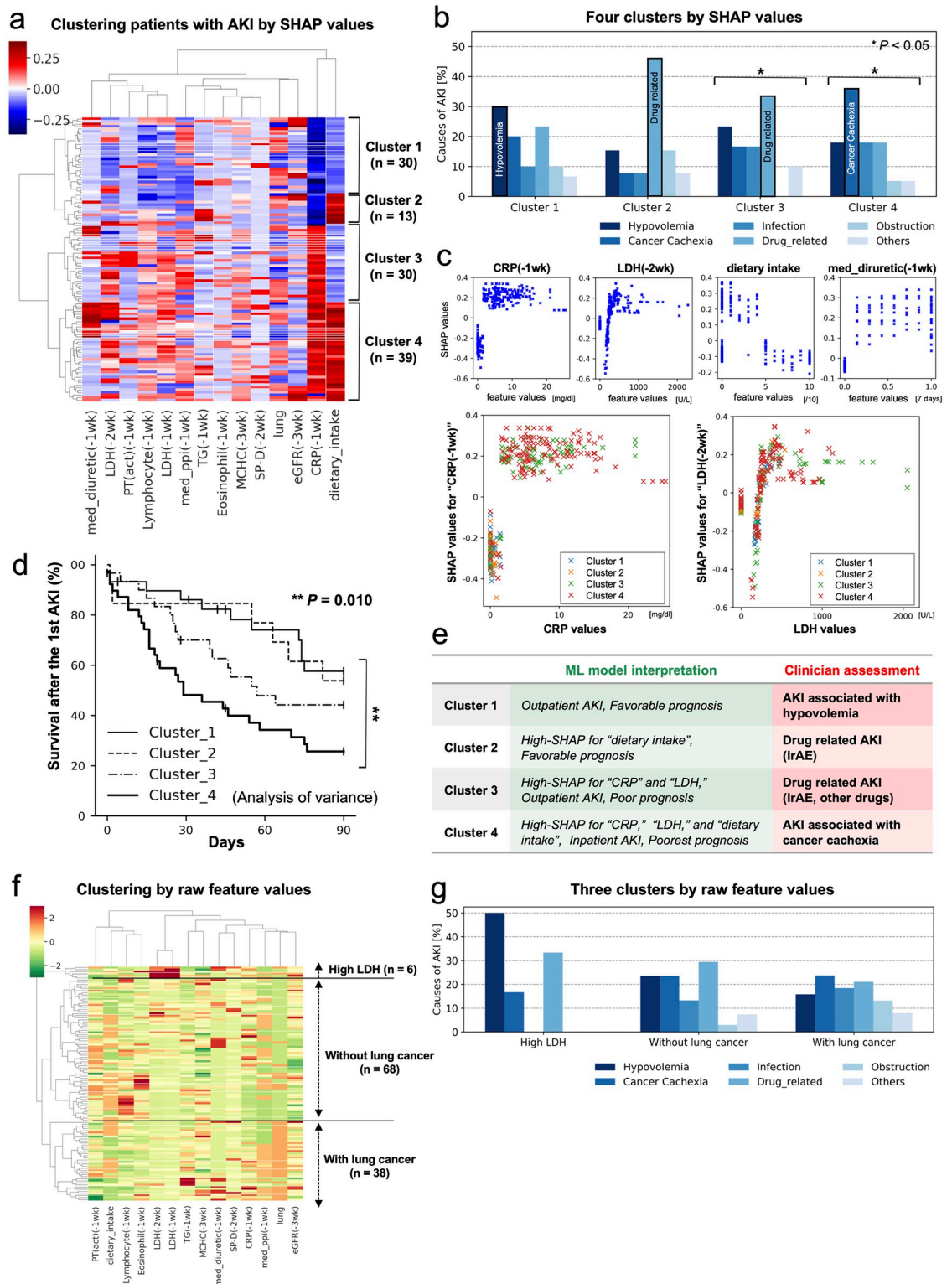


Fig 3. (a) Patient clustering by SHAP values. Overall, 112 patients with AKI were categorized into four clusters with ML-based unsupervised clustering by SHAP values. The number of clusters was determined as the number of visually valid clusters indicated on the dendrogram. (b) Distribution of annotations for causes of AKI in the four clusters. The distribution of annotation labels was calculated cluster-wise. (c) Dependence plot of key features. Each point in the scatterplot reveals the correlation between the values of key features and SHAP in the last week prior to each AKI development among 112 patients. The plots in the features of CRP and

LDH are color-coded by cluster. (d) Survival analysis after AKI. Kaplan—Meier curves of 90-day survival after the first AKI in each cluster. Analysis of variance reveals significant differences in survival rates among the four clusters, with Cluster 4 having the poorest prognosis. (e) Interpretation of the AI model and clinician assessment. The interpretation of the AI-based model is indicated by patient clustering based on predictive reasoning and prognostic variance. Clinician assessment is indicated by the reviews of nephrologists. (f) Patient clustering by raw feature values. Clustering by raw values of the key features, excluding SHAP weighting, categorizes the same patients with AKI into three clusters. (g) Distribution of annotations for causes of AKI in the three clusters. As in (b), six labels were aggregated for each cluster with the contributing factors for AKI. Clustering by raw values of the key features does not provide meaningful patient clustering reflecting the clinical background of AKI. SHAP, SHapley Additive exPlanations; AKI, acute kidney injury; CRP, C-reactive protein; LDH, Lactate Dehydrogenase; med_diuretic(-1wk), medication of diuretics within the last week.

<https://doi.org/10.1371/journal.pone.0298673.g003>

poor dietary intake are associated with organ damage and dehydration, which can be causes of AKI in advanced cancers [4]. According to the chart review by nephrologists, certain patients with AKI in cluster 4 had cancer cachexia in the terminal phase, while some developed diuretic-induced AKI. Based on these findings, the AKI predictive reasoning in cluster 4 can be interpreted as “patients with terminal cancer and cachexia who developed AKI due to worsening conditions or diuretic use, high CRP and LDH levels, and poor dietary intake.” In

Table 2. Clinical characteristics of patients with acute kidney injury in each cluster.

	Cluster 1	Cluster 2	Cluster 3	Cluster 4	p-value
Number of patients [n]	30	13	30	39	
Age [n (%)]					
20–39 years	0 (0)	1 (8)	0 (0)	2 (5)	0.203
40–59 years	6 (20)	2 (15)	8 (27)	5 (13)	0.590
60–79 years	21 (70)	9 (69)	20 (67)	30 (77)	0.720
> 80 years	3 (10)	1 (8)	2 (7)	2 (5)	0.953
Male [n] / Female [n]	22 / 8	7 / 6	19 / 11	34 / 5	< 0.05 *
Malignancy types [n (%)]					
Gastrointestinal	4 (13)	1 (8)	4 (13)	1 (2)	0.262
Lung	10 (33)	5 (38)	14 (47)	16 (41)	0.780
Urologic	8 (27)	5 (38)	3 (10)	7 (18)	0.108
Skin	7 (23)	1 (8)	8 (27)	12 (31)	0.492
Other	1 (3)	1 (8)	1 (3)	3 (8)	0.730
Baseline SCr [mg/dL, median (IQR)]	0.91 (0.77–1.12)	0.75 (0.62–1.32)	0.85 (0.62–0.99)	0.92 (0.73–1.18)	0.543
AKI stage on first episode of AKI [n (%)]					
Stage 1	19 (63)	8 (62)	27 (90)	26 (67)	< 0.05 *
Stage 2	6 (20)	3 (23)	2 (7)	8 (20)	0.322
Stage 3 or require RRT	5 (17)	2 (15)	1 (3)	5 (13)	0.343
Ratio of inpatient AKI [n (%)]	3 (10)	6 (46)	7 (23)	36 (92)	< 0.05 *
Primary cause of AKI [n (%)]					
Hypovolemia	9 (30)	2 (15)	7 (23)	7 (18)	0.634
Cancer Cachexia	6 (20)	1 (8)	5 (17)	14 (36)	0.125
Infection	3 (10)	1 (8)	5 (17)	7 (18)	0.765
Drug-related	7 (23)	6 (46)	10 (33)	7 (18)	0.174
Obstruction	3 (10)	2 (15)	0 (0)	2 (5)	0.142
Others	2 (7)	1 (8)	3 (10)	2 (5)	0.953

All data are presented as medians (interquartile range, IQR) or means (standard deviation, SD), as appropriate for nonparametric or parametric variables, respectively. Comparisons of categorical variables and means among clusters are made using Fisher’s exact probability test and the Kruskal—Wallis test, respectively. AKI, acute kidney injury; ICI, immune checkpoint inhibitors; SCr, serum creatinine; RRT, renal replacement therapy; IQR, interquartile range; SD, standard deviation.

<https://doi.org/10.1371/journal.pone.0298673.t002>

addition, when the dependence plots of CRP and LDH were color-coded by cluster, higher values of the features and SHAP were frequently observed in clusters 3 and 4 (Fig 3c). Furthermore, since the clustering with AKI predictive reasoning captured the distinct clinical characteristics of cancer patients, we speculated that patient clustering by SHAP may capture prognostic differences in advanced cancers. Therefore, the 90-day survival rate of 112 patients with the first occurrence of AKI was analyzed, and it was discovered that significant prognostic differences existed between the four clusters (Fig 3d). Notably, cluster 4 had the poorest prognosis. These findings suggest that the predictive reasoning for AKI can recognize prognostic variances after AKI, supporting the clinical validity of patient clustering by SHAP (Fig 3e).

To confirm the necessity of SHAP in clinical interpretation, the same patients were clustered by the raw values for the same key features and divided into three clusters (Fig 3f). The results revealed that, in contrast to SHAP clustering, there were no distinguishing characteristics in the causes of AKI between the clusters, and each cluster did not reflect the contributing risk factors for AKI development (Fig 3g).

Among the patients in clusters 2 and 3, only a few cases of suspected ICI or IrAE involvement were confirmed on renal biopsy. A detailed chart review revealed that many cases were not biopsied for AKI diagnosis after discussions among the attending physician, patient, and their family; consideration of the general condition of the procedure; the prognosis of the patient; and the risk of fatal complications.

Discussion

Herein, we have shown that the clustering approach using SHAP values in ML-based AKI prediction models offers a novel perspective in assessing the etiology of each episode of AKI in patients undergoing ICI therapy. Patient clustering based on time-series SHAP values for AKI prediction enables clinicians to interpret predictive reasoning that reflects the underlying causes of AKI individually. This indicates that we can infer factors critical for AKI development on a case specific basis by focusing on the temporal changes and patterns in each SHAP value in the ML model, which continuously predicts AKI. Therefore, our approach seems appropriate for estimating the most critical causes of AKI in cancer patients receiving systemic therapy, including ICI therapy, with diverse and complicated AKI risks. The features predicted as particularly essential variables in our model were consistent with the findings of previous studies using multivariate analyses [11–15]. PPIs, which have been associated with the development of AKI in several observational studies [12, 13, 30], were also identified as a key feature in our prediction model. In addition, although not at the top of the list, diuretics, NSAIDs, and baseline renal function features were also identified as key risk factors by the model, as shown in the dependence plot [17] (Fig 3c, S4 Fig in S1 File). Although the dependence plot did not indicate a causal relationship, the prediction model regarded these key features as crucial for predicting AKI.

However, our method identified individual differences in the underlying backgrounds of AKI that could not have been deduced by conventional methods. As indicated by the varying distribution of clinician annotations (Fig 3b), the patient clusters classified based on the predicted key features had different AKI development backgrounds; for example, cluster 4 was interpreted to have cancer cachexia as the primary contributing factor to AKI development, whereas clusters 2 and 3 suggested the contribution of drugs, including ICI or IrAE. Patients in cluster 4 were characterized by high CRP and LDH levels and the use of diuretics and had the poorest prognosis after the development of AKI (Fig 3c and 3d). These predictive findings reflect the development of AKI due to cancer cachexia. Cluster 3 had more cases of higher CRP levels, persistent inflammation due to IrAE, infections, and end-stage cancer, with many

patients receiving outpatient follow-ups. The high SHAP trend of CRP in cluster 3 was considered reflective of these conditions. In contrast, cluster 2 had relatively more cases of poor dietary intake that required hospitalization and fever. The high SHAP trend of dietary intake in cluster 2 was considered to reflect these conditions. Most patients with drug-related AKI in clusters 2 and 3 developed extra-renal IrAEs before AKI [15] (S2 Table in [S1 File](#)). In addition, significant prognostic differences were noted between the clusters according to the predictive reasoning, although no variable for survival was provided for model training. This indicates that the predictive reasoning of the AI model is not solely derived from a combination of laboratory values and medications. Although some studies have discussed the prognostic relevance of AKI in ICI-treated patients [11, 13, 14], our study suggested that prognostic differences after AKI were relevant regarding the differences in predicted factors of AKI development.

In several AI-based prediction models, SHAP has been widely used to predict risk factors for various outcomes, including AKI [31–34]. However, although it is possible to infer predicted characteristics that demonstrate measurable correlations with SHAP values, it has not been feasible to determine their clinical significance in individual patients. This is partly because the correlation between an individual input feature and its contribution does not fully explain the pathophysiology of complicated outcomes. Furthermore, although many features with nonlinear relationships with SHAP values contribute to the prediction of AKI (S4 Fig in [S1 File](#)), comprehending the clinical importance of each feature with a nonlinear contribution is challenging. To the best of our knowledge, no study has attempted to clinically interpret the meaning of contributing factors as individual risk factors in each patient. We found that the combination of contributing factors, including nonlinear contributions, constitutes predictive reasoning in AI models representing the time-varying AKI risks. This method allowed us to clinically interpret the underlying background behind individualized prediction of AKI observed in different time series for the first time.

We believe that our study is significant because it reveals underlying causes in individual patients with AKI in ICI therapy, which cannot be obtained by conventional approaches, and provides predictive reasoning with clinically valid interpretability. However, the implications of our study go beyond simply allowing individualized assessment of AKI during ICI therapy. Cancer patients typically develop AKI owing to complex risk factors arising from various medications or complications. Therefore, predicting AKI development by monitoring a single laboratory result or medication considered as critical factors is often difficult. Similar to investigating the significant contributive features by SHAP analysis, determining the most critical factor for AKI among the multilayered AKI risk factors is a process that clinicians implement to select patients at high risk of AKI and assess their risks. Clinicians usually follow thought processes such as “the probability of AKI onset increases when additional risk factors such as infections and diuretics (triggers) are added to the background of cancer cachexia (underlying risks).” When interpreting the combination of underlying clinical backgrounds and additional stratified risks that lead to AKI development, analyzing the individual AI models’ predictive reasoning can be a valuable approach to explore the most critical AKI risks, which are challenging to understand using routine medical data [35]. In the future, this approach will help effectively determine the appropriate assessment and intervention for patients with complicated AKI risks (S5 Fig in [S1 File](#)) [36]. Further analyses applying a similar approach to patients receiving other chemotherapy may capture other characteristic predicting reasoning models specific to the causative agent and disease state. Furthermore, this model can be applied to predict AKI and other outcomes in various other fields that need such individualized prediction.

This study had several limitations. First, this model was developed at a single center; hence, multicenter studies are needed for external validation. Second, due to the nature of ICI

therapy, the difference in data availability may have affected the prediction accuracy and the contribution of the features (S6 Fig in [S1 File](#)). Therefore, designing equal time-series features, devising missing interpolations, and selecting the population may resolve this problem. Third, information on image findings and surgery, which may be necessary for specific AKI prediction (e.g., obstructive AKI), were not included as features in the present model. Therefore, adding such information in future studies can further improve the performance and interpretability of the model. Furthermore, the validity of the clinical interpretation was assessed by reviews conducted by nephrologists; however, information may have been missed in the retrospective chart reviews. Finally, although this was a retrospective analysis by design, future prospective studies are expected to clarify the benefits of patient clustering by predictive reasoning, which can aid clinicians' decisions and patient outcomes by prospectively predicting new patients with AKI.

In conclusion, the study findings are significant as this study is the first to demonstrate a novel approach for interpreting ML models by patient clustering using individual predictive reasoning patterns and has the potential to accelerate future medical applications of AI. We expect our approach to be widely applied to explainable AI in various medical fields, including renal diseases.

Supporting information

S1 File. Contains all the supporting files.
(PDF)

Acknowledgments

We thank Tomohiro Kuroda and the Division of Medical Informatics and Administration Planning, Kyoto University Hospital, for the EMR data extraction and management. We also like to thank Editage (www.editage.com) for English language editing.

Author Contributions

Conceptualization: Minoru Sakuragi.

Data curation: Minoru Sakuragi, Eiichiro Uchino, Noriaki Sato.

Formal analysis: Minoru Sakuragi.

Funding acquisition: Yasushi Okuno.

Investigation: Minoru Sakuragi.

Methodology: Minoru Sakuragi, Eiichiro Uchino, Noriaki Sato.

Project administration: Motoko Yanagita, Yasushi Okuno.

Resources: Motoko Yanagita, Yasushi Okuno.

Software: Minoru Sakuragi, Eiichiro Uchino, Ryosuke Kojima.

Supervision: Motoko Yanagita, Yasushi Okuno.

Validation: Takeshi Matsubara, Akihiko Ueda, Yohei Mineharu.

Visualization: Minoru Sakuragi.

Writing – original draft: Minoru Sakuragi.

Writing – review & editing: Eiichiro Uchino, Noriaki Sato, Takeshi Matsubara, Akihiko Ueda, Yohei Mineharu, Motoko Yanagita, Yasushi Okuno.

References

1. Lam AQ, Humphreys BD. Onco-nephrology: AKI in the cancer patient. *Clin J Am Soc Nephrol*. 2012; 7: 1692–1700. <https://doi.org/10.2215/CJN.03140312> PMID: 22879433
2. Salahudeen AK, Doshi SM, Pawar T, Nowshad G, Lahoti A, Shah P. Incidence rate, clinical correlates, and outcomes of AKI in patients admitted to a comprehensive cancer center. *Clin J Am Soc Nephrol*. 2013; 8: 347–354. <https://doi.org/10.2215/CJN.03530412> PMID: 23243268
3. Cohen EP, Krzesinski JM, Launay-Vacher V, Sprangers B. Onco-nephrology: core curriculum 2015. *Am J Kidney Dis*. 2015; 66: 869–883. <https://doi.org/10.1053/j.ajkd.2015.04.042> PMID: 26060184
4. Postow MA, Sidlow R, Hellmann MD. Immune-related adverse events associated with immune checkpoint blockade. *N Engl J Med*. 2018; 378: 158–168. <https://doi.org/10.1056/NEJMra1703481> PMID: 29320654
5. Shingarev R, Glezerman IG. Kidney complications of immune checkpoint inhibitors: a review. *Am J Kidney Dis*. 2019; 74: 529–537. <https://doi.org/10.1053/j.ajkd.2019.03.433> PMID: 31303350
6. Cortazar FB, Marrone KA, Troxell ML, Raito KM, Hoenig MP, Brahmer JR, et al. Clinicopathological features of acute kidney injury associated with immune checkpoint inhibitors. *Kidney Int*. 2016; 90: 638–647. <https://doi.org/10.1016/j.kint.2016.04.008> PMID: 27282937
7. Shirali AC, Perazella MA, Gettinger S. Association of acute interstitial nephritis with programmed cell death 1 Inhibitor Therapy in Lung Cancer Patients. *Am J Kidney Dis*. 2016; 68: 287–291. <https://doi.org/10.1053/j.ajkd.2016.02.057> PMID: 27113507
8. Mamlouk O, Selamet U, Machado S, Abdelrahim M, Glass WF, Tchakarov A, et al. Nephrotoxicity of immune checkpoint inhibitors beyond tubulointerstitial nephritis: single-center experience. *J Immunother Cancer*. 2019; 7: 2. <https://doi.org/10.1186/s40425-018-0478-8> PMID: 30612580
9. Koks MS, Ocak G, Suelmann BBM, Hulsbergen-Veelken CAR, Haitjema S, Vianen ME, et al. Immune checkpoint inhibitor-associated acute kidney injury and mortality: an observational study. *PLOS ONE*. 2021; 16: e0252978. <https://doi.org/10.1371/journal.pone.0252978> PMID: 34101756
10. Shimamura Y, Watanabe S, Maeda T, Abe K, Ogawa Y, Takizawa H. Incidence and risk factors of acute kidney injury, and its effect on mortality among Japanese patients receiving immune check point inhibitors: a single-center observational study. *Clin Exp Nephrol*. 2021; 25: 479–487. <https://doi.org/10.1007/s10157-020-02008-1> PMID: 33471239
11. García-Carro C, Bolufer M, Bury R, Castañeda Z, Muñoz E, Felip E, et al. Acute kidney injury as a risk factor for mortality in oncological patients receiving checkpoint inhibitors. *Nephrol Dial Transplant*. 2022; 37: 887–894. <https://doi.org/10.1093/ndt/gfab034> PMID: 33547795
12. Seethapathy H, Zhao S, Chute DF, Zubiri L, Oppong Y, Strohehn I, et al. The incidence, causes, and risk factors of acute kidney injury in patients receiving immune checkpoint inhibitors. *Clin J Am Soc Nephrol*. 2019; 14: 1692–1700. <https://doi.org/10.2215/CJN.00990119> PMID: 31672794
13. Cortazar FB, Kibbelaar ZA, Glezerman IG, Abudayyeh A, Mamlouk O, Motwani SS, et al. Clinical features and outcomes of immune checkpoint inhibitor-associated Aki: A multicenter Study. *J Am Soc Nephrol*. 2020; 31(2020): 435–446. <https://doi.org/10.1681/ASN.2019070676> PMID: 31896554
14. Meraz-Muñoz A, Amir E, Ng P, Avila-Casado C, Ragobar C, Chan C, et al. Acute kidney injury associated with immune checkpoint inhibitor therapy: incidence, risk factors and outcomes. *J Immunother Cancer*. 2020; 8: e000467. <https://doi.org/10.1136/jitc-2019-000467> PMID: 32601079
15. Gupta S, Short SAP, Sise ME, Prosek JM, Madhavan SM, Soler MJ, et al. Acute kidney injury in patients treated with immune checkpoint inhibitors. *J Immunother Cancer*. 2021; 9: e003467. <https://doi.org/10.1136/jitc-2021-003467> PMID: 34625513
16. Gérard AO, Barbosa S, Parassol N, Andreani M, Merino D, Cremoni M, et al. Risk factors associated with immune checkpoint inhibitor—induced acute kidney injury compared with other immune-related adverse events: a case—control study. *Clin Kidney J*. 2022; 15(10): 1881–1887. <https://doi.org/10.1093/ckj/sfac109> PMID: 36158153
17. Ji MS, Wu R, Feng Z, Wang YD, Wang Y, Zhang L, et al. Incidence, risk factors and prognosis of acute kidney injury in patients treated with immune checkpoint inhibitors: a retrospective study. *Sci Rep*. 2022; 12: 18752. <https://doi.org/10.1038/s41598-022-21912-y> PMID: 36335144
18. Lundberg SM, Erion G, Chen H, DeGrave A, Prutkin JM, Nair B, et al. From local explanations to global understanding with explainable AI for trees. *Nat Mach Intell*. 2020; 2: 56–67. <https://doi.org/10.1038/s42256-019-0138-9> PMID: 32607472

19. Kellum JA, Lameire N, Aspelin P, Barsoum RS, Burdmann EA, Goldstein SL, et al. Kidney disease: improving global outcomes (KDIGO) acute kidney injury work group. KDIGO clinical practice guideline for acute kidney injury. *Kidney Int Suppl.* 2012; 2: 1–138.
20. Ke G, Meng Q, Finley T, Wang T, Chen W, Ma W, et al. LightGBM: A highly efficient gradient boosting decision tree, NIPS 2017. 30; 2017: pp. 3149–3157. Available from: <https://papers.nips.cc/paper/6907-lightgbm-a-highly-efficient-gradientboosting-decision-tree.pdf>.
21. Pedregosa F, Varoquaux G, Gramfort A, Michel V, Thirion B, Grisel O, et al. Scikit-learn: Machine Learning in Python. *J Mach Learn Res.* 2011; 12: 2825–2830.
22. Wu L, Hu Y, Liu X, Zhang X, Chen W, Yu ASL, et al. Feature ranking in predictive models for hospital-acquired acute kidney injury. *Sci Rep.* 2018; 8: 17298. <https://doi.org/10.1038/s41598-018-35487-0> PMID: 30470779
23. Koyner JL, Carey KA, Edelson DP, Churpek MM. The development of a machine learning inpatient acute kidney injury prediction model. *Crit Care Med.* 2018; 46: 1070–1077. <https://doi.org/10.1097/CCM.0000000000003123> PMID: 29596073
24. He J, Hu Y, Zhang X, Wu L, Waitman LR, Liu M. Multi-perspective predictive modeling for acute kidney injury in general hospital populations using electronic medical records. *JAMIA Open.* 2019; 2: 115–122. <https://doi.org/10.1093/jamiaopen/ooy043> PMID: 30976758
25. Tomašev N, Glorot X, Rae JW, Zielinski M, Askham H, Saraiva A, et al. A clinically applicable approach to continuous prediction of future acute kidney injury. *Nature.* 2019; 572: 116–119. <https://doi.org/10.1038/s41586-019-1390-1> PMID: 31367026
26. Wu L, Hu Y, Zhang X, Chen W, Yu ASL, Kellum JA, et al. Changing relative risk of clinical factors for hospital-acquired acute kidney injury across age groups: a retrospective cohort study. *BMC Nephrol.* 2020; 21: 321. <https://doi.org/10.1186/s12882-020-01980-w> PMID: 32741377
27. Rank N, Pfahringer B, Kempfert J, Stamm C, Kühne T, Schoenrath F, et al. Deep-learning-based real-time prediction of acute kidney injury outperforms human predictive performance. *npj Digit Med.* 2020; 3: 139. <https://doi.org/10.1038/s41746-020-00346-8> PMID: 33134556
28. Park N, Kang E, Park M, Lee H, Kang HG, Yoon HJ, et al. Predicting acute kidney injury in cancer patients using heterogeneous and irregular data. *PLOS ONE.* 2018; 13: e0199839. <https://doi.org/10.1371/journal.pone.0199839> PMID: 30024918
29. Sandokji I, Yamamoto Y, Biswas A, Arora T, Ugwuowo U, Simonov M, et al. A time-updated, parsimonious model to predict AKI in hospitalized children. *J Am Soc Nephrol.* 2020; 31: 1348–1357. <https://doi.org/10.1681/ASN.2019070745> PMID: 32381598
30. Abdelrahim M, Mamlouk O, Lin H, Lin J, Page V, Abdel-Wahab N, et al. Incidence, predictors, and survival impact of acute kidney injury in patients with melanoma treated with immune checkpoint inhibitors: a 10-year single-institution analysis. *Oncoimmunology.* 2021; 10: 1927313. <https://doi.org/10.1080/2162402X.2021.1927313> PMID: 34104543
31. Lauritsen SM, Kristensen M, Olsen MV, Larsen MS, Lauritsen KM, Jørgensen MJ, et al. Explainable artificial intelligence model to predict acute critical illness from electronic health records. *Nat Commun.* 2020; 11: 3852. <https://doi.org/10.1038/s41467-020-17431-x> PMID: 32737308
32. Zhang Y, Yang D, Liu Z, Chen C, Ge M, Li X, et al. An explainable supervised machine learning predictor of acute kidney injury after adult deceased donor liver transplantation. *J Transl Med.* 2021; 19: 321. <https://doi.org/10.1186/s12967-021-02990-4> PMID: 34321016
33. Shakeri E, Mohammed EA, Shakeri HAZ, Far B. Exploring features contributing to the early prediction of sepsis using machine learning, annu. Int. Conf. IEEE Eng Med Biol Soc 2021 (20241). pp. 2472–2475.
34. Monsarrat P, Bernard D, Marty M, Cecchin-Albertoni C, Doumard E, Gez L, et al. Systemic periodontal risk score using an innovative machine learning strategy: an observational study. *J Pers Med.* 2022; 12: 217. <https://doi.org/10.3390/jpm12020217> PMID: 35207705
35. Beaulieu-Jones BK, Yuan W, Brat GA, Beam AL, Weber G, Ruffin M, et al. Machine learning for patient risk stratification: standing on, or looking over, the shoulders of clinicians? *npj Digit Med.* 2021; 4: 62. <https://doi.org/10.1038/s41746-021-00426-3> PMID: 33785839
36. Yang CC. Explainable artificial intelligence for predictive modeling in healthcare. *J Healthc Inform Res.* 2022; 6: 228–239. <https://doi.org/10.1007/s41666-022-00114-1> PMID: 35194568

SUPPORTING INFORMATION

Interpretable machine learning-based individual analysis of acute kidney injury in immune checkpoint inhibitor therapy

Minoru Sakuragi, Eiichiro Uchino, Noriaki Sato, Takeshi Matsubara, Akihiko Ueda, Yohei Mineharu, Ryosuke Kojima, Motoko Yanagita, and Yasushi Okuno.

Table of Contents

I. SUPPORTING METHODS

S1 Method. Definition of acute kidney injury

S2 Method. Details of the input features

S3 Method. Annotation by nephrologists

II. SUPPORTING FIGURES

S1 Fig. Construction of the dataset from the EMR data of each patient

S2 Fig. Labeled training data

S3 Fig. Visualizing individual AKI predictive reasoning and clustering

S4 Fig. Dependence plot of key features among 112 patients with AKI

S5 Fig. Example of the future application of individual predictive reasoning

S6 Fig. Prediction Probabilities in each cluster

S7 Fig. Precision-Recall curve and calibration plot

III. SUPPORTING TABLES

S1 Table. Comparative performance of various machine learning models

S2 Table. Details of “Drug-related AKI Causes” by annotation in Clusters 2 and 3

S3 Table. Details of “Other AKI Causes” by annotation

S1 Method. Definition of acute kidney injury

For the detection of acute kidney injury (AKI), the following Kidney Disease Improving Global Outcomes

(KDIGO) definition,^{S1} excluding the urine output criteria, was employed:

- ≥ 0.3 mg/dL increase in serum creatinine (SCr) levels within 48 h

OR

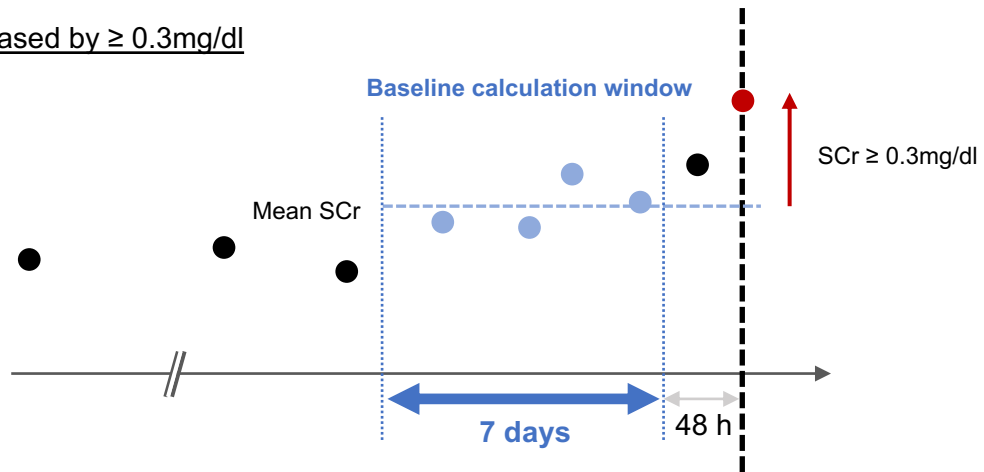
- ≥ 1.5 -fold increase in SCr levels over baseline within 7 days

OR

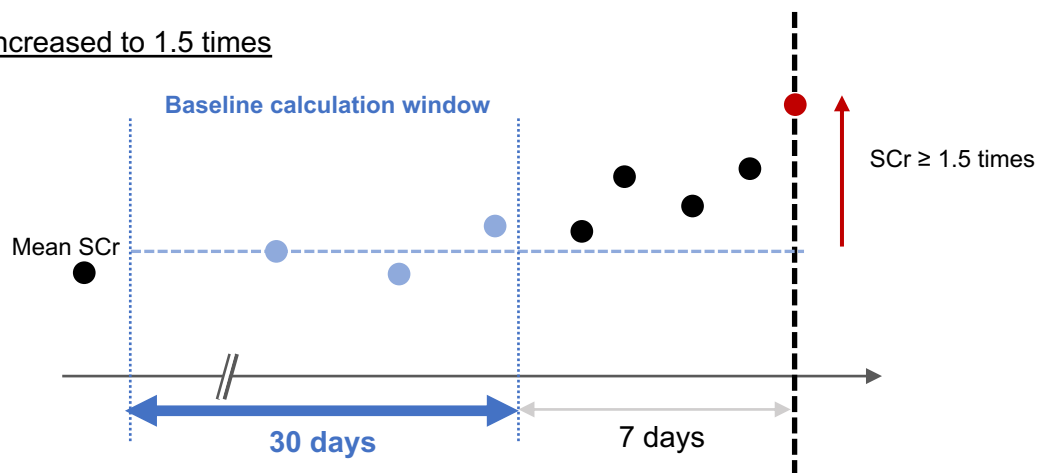
- initiation of renal replacement therapy

The mean SCr values in the 7- and 30-day baseline calculation windows were calculated using the criterion of 0.3 mg/dL or 1.5 times (illustrated below). SCr values can gradually increase before meeting the AKI criteria; therefore, values within 48 h and 7 days prior to the reference time point were excluded from the respective mean value calculations to avoid overestimation of baseline SCr values.

Increased by $\geq 0.3\text{mg/dl}$



Increased to 1.5 times



S2 Method. Details of the input features

1. Demographics

A total of two features were employed: the latest values for (1) sex and (2) age. Information on age was aggregated into four characteristics, “20–39 years,” “40–59 years,” “60–79 years,” and “80 years and older,” and used as categorical variables.

2. Disease name

A total of five features were established according to the 10th revision of the International Statistical Classification of Diseases (ICD-10) code, and the names of malignant tumors beginning with the code “C” in ICD-10 were aggregated into six disease names: “Gastrointestinal malignancies,” “Lung malignancies,” “Urologic malignancies,” “Skin malignancies,” and “Other malignancies.”

3. Vital signs

Three items were used: pulse rate, urinary volume, and mean artery pressure (MAP). If MAP values were not available, they were calculated from systolic (SBP) and diastolic (DBP) blood pressure values using the formula: $MAP = 1/3 \times SBP + 2/3 \times DBP$.

4. Dietary intake

Based on the information from a 10-point scale from electronic medical records (EMRs), the dietary intake for the past 7 days from the reference time point was represented as a 10-point scale. The information on “fasting” and “no dietary intake” was entered as 0. The absence of dietary information was regarded as a missing value.

5. Laboratory data

Fifty-two common characteristics of the blood samples were used. Laboratory features had selected items, with less than half missing in the measured data of the patients included in the study. These 52 items had time-series information, and rolling features were generated every 7 days for the past 28 days from the prediction timepoint as the lag variable (see Supplementary Figure S2). The SCr at the start of immune checkpoint inhibitors (ICI) administration was used as “basal_SCr” as one of the patient-specific information.

Items by blood test with time-series information

ACTH (Adrenocorticotrophic hormone)	Ca (Calcium)	K (Potassium)	SP-D (Supply Processing and Distribution)
ALB (Albumin)	Ch-E (cholinesterase)	KL-6 (Sialylated carbohydrate antigen KL-6)	T-Bil (Total bilirubin),
ALP (Alkaline phosphatase)	Cl (Chloride)	LDH (Lactate dehydrogenase)	T-CHO (Total cholesterol)
ALT (Alanine aminotransferase)	Eosinophil	Lymphocyte	TG (Triglyceride)
AMY (Amylase)	FIB (Fibrinogen)	MCH (Mean corpuscular hemoglobin)	TP (Total protein)
APTT (activated partial thromboplastin time)	FT3 (Free triiodothyronine)	MCHC (Mean corpuscular hemoglobin concentration)	TSH (Thyroid-stimulating hormone)
AST (Aspartate aminotransferase)	FT4 (Free thyroxine)	MCV (Mean corpuscular volume)	UA (Uric acid)
BG (Blood glucose)	HCT (Hematocrit)	Monocyte	WBC (White blood cell)

BUN (Blood urea nitrogen)	HGB (Hemoglobin)	Na (Sodium)	Cortisol
Basophil	HbA1c (Hemoglobin A1c)	Neutrophil	eGFR (estimated glomerular filtration rate)
CK (Creatinine kinase)	HbF (Hemoglobin F)	PLT (Platelet)	gGTP (γ -glutamyl transpeptidase)
CRE (Creatinine)	IP (Inorganic phosphorus)	PT act (prothrombin time)	sBG (Serum blood glucose)
CRP (C-reactive protein)	IgG (Immunoglobulin-G)	RBC (Red blood cell)	D-dimer

Values for windows without measurements were interpolated for vital signs and laboratory data. Linear interpolation was performed if values were obtained before or after a window in which no measurements were taken 7 days prior to the reference time point; feed-forward or feed-back methods were employed.

6. Medication

Sixteen types of medication information (oral and injectable) were used as features. Oral medications included antibiotics, diuretics, proton pump inhibitors (PPIs), nonsteroidal anti-inflammatory drugs (NSAIDs), acetaminophen, angiotensin-converting enzyme inhibitors (ACE-I)/angiotensin II receptor blocker (ARB), and steroids. Injectable drugs included antibiotics, diuretics, PPIs, NSAIDs, acetaminophen, steroids, anticancer agents, contrast media, and ICI. Each medication information was entered as 0, 1/7, 2/7, ... 6/7, and 1 based on the number of days administered for the past 7 days from the prediction time point.

S3 Method. Annotation by nephrologists

For the 112 eligible ICI-treated patients who developed AKI, three nephrologists independently conducted chart reviews and free-text annotations of factors contributing to AKI development. Each nephrologist performed the chart review based entirely on their clinical experience without being informed of the results of the prediction model, the reasons for individual predictions, or the results of patient clustering by SHAP (SHapley Additive exPlanations).

The annotation content was classified into six categories according to keywords and rules.

Hypovolemia:

- With keywords such as “dehydration,” “prerenal,” “poor dietary intake,” “fluid loss,” and “shock,” or annotations of “deterioration of general condition with infection” or “deterioration of general condition with wasting.”

Cachexia:

- With keywords such as “terminal,” “cancer ascites,” and “cancer pleural effusion,” or annotations of “wasting due to cancer and malnutrition.”

Infection:

- With keywords such as “sepsis,” “infection,” or annotation of “infection.”

Obstruction:

- With keywords such as “post-renal” and “hydronephrosis.”

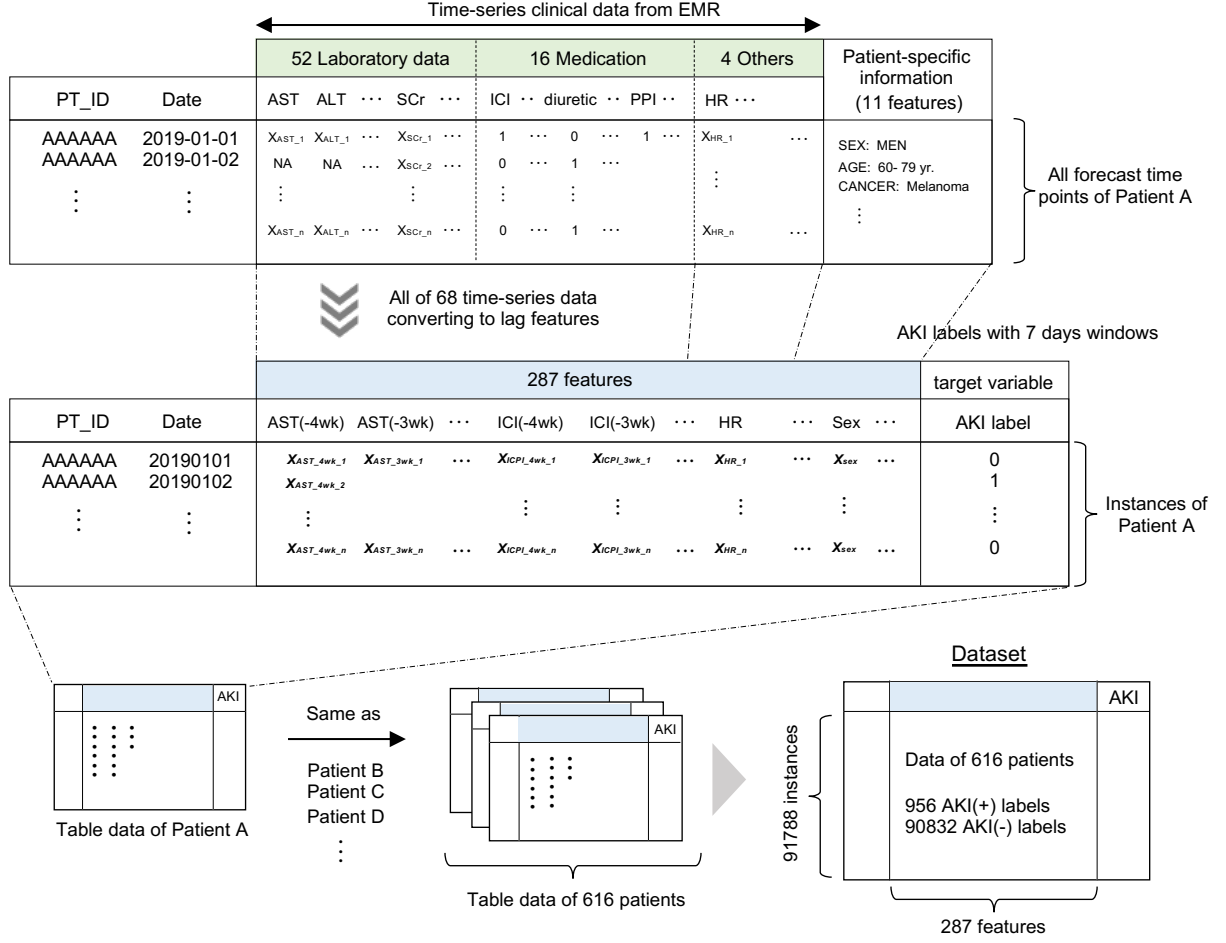
Drug-related:

- With keywords such as “drug-related,” “diuretics,” “ARB,” “antibiotics,” “immune-related adverse events (IrAE),” and “ICI,” or annotations such as “drug-related,” “due to ICI,” and “with IrAE.”

Others:

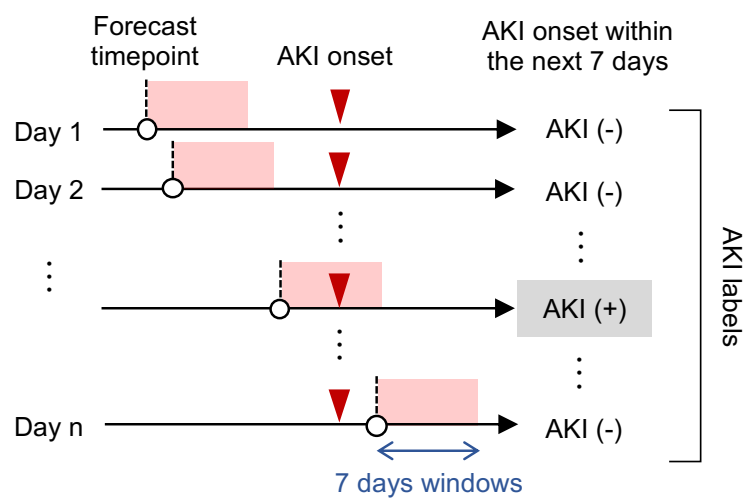
- Factors that do not apply to any of the aforementioned categories.

Each patient’s annotation result was assigned one of the six aforementioned labels. If more than one label was applicable, the label of the most dominant factor was adopted from the description.



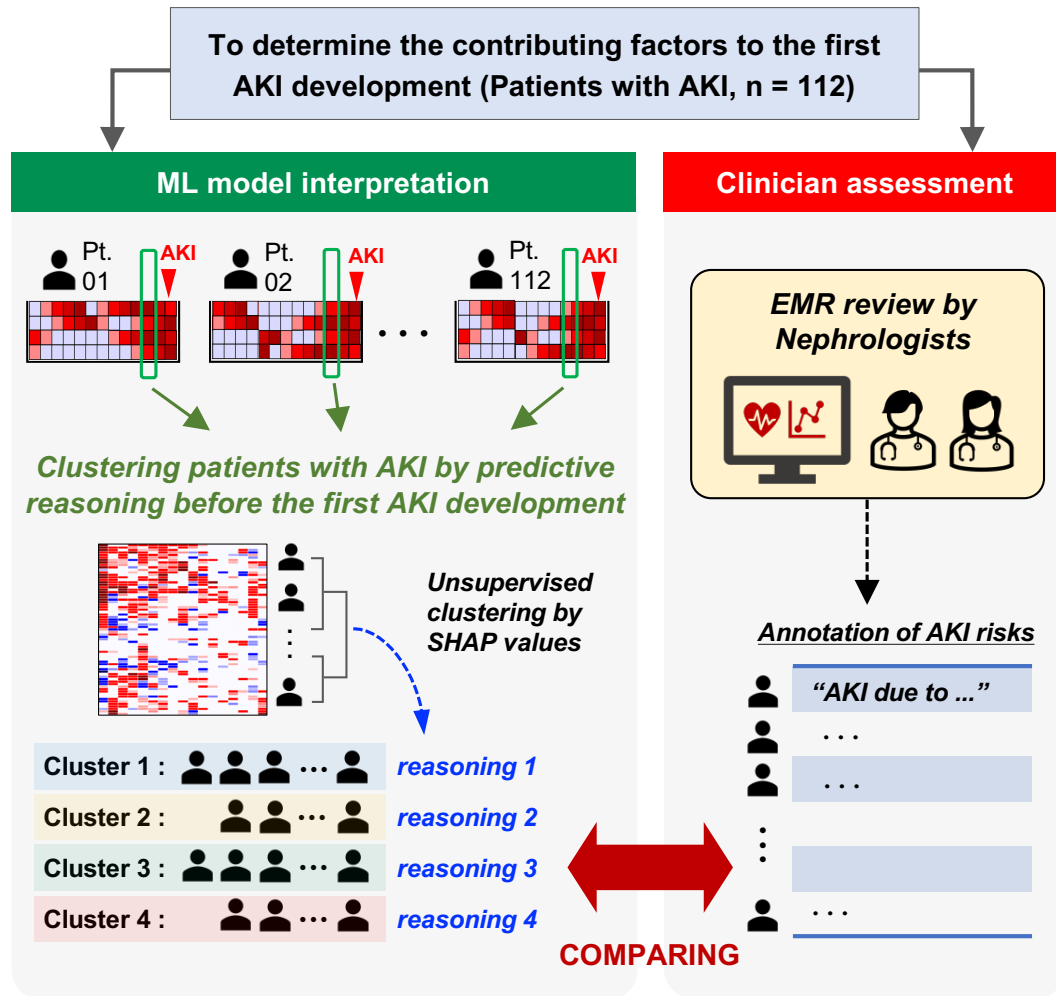
S1 Fig. Construction of the dataset from the EMR data of each patient

All time-series clinical data were converted to lag features with a 7-day window (i.e., “AST (-4 wk),” “AST (-3 wk),” “AST (-2 wk),” “AST (-1 wk)”). Laboratory (52 items) and medication (16 items) data with time-series information were transformed into features-rolling data every 7 days for the past 28 days from the time of prediction as lag variables. The three vital signs and dietary intake data were used as time-series information without rolling, and the three types of patient-specific information (10 items) other than “basal_SCr” were used as categorical variables. EMR, electronic medical record; AST, aspartate aminotransferase.



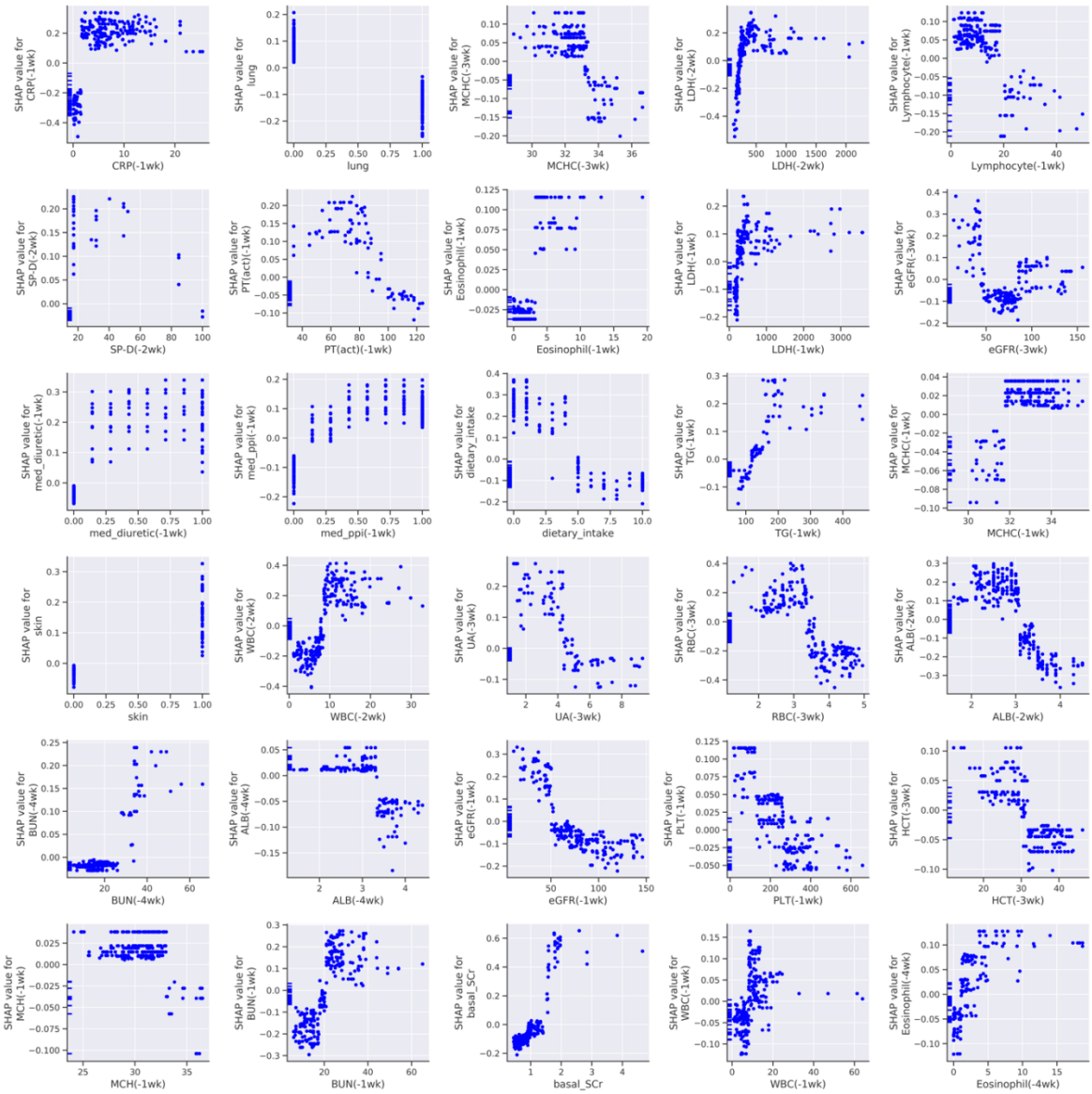
S2 Fig. Labeled training data

AKI-positive indicates occurrence of AKI within a 7-day forecast window. AKI development after 14 days was excluded from this labeling. AKI, acute kidney injury.



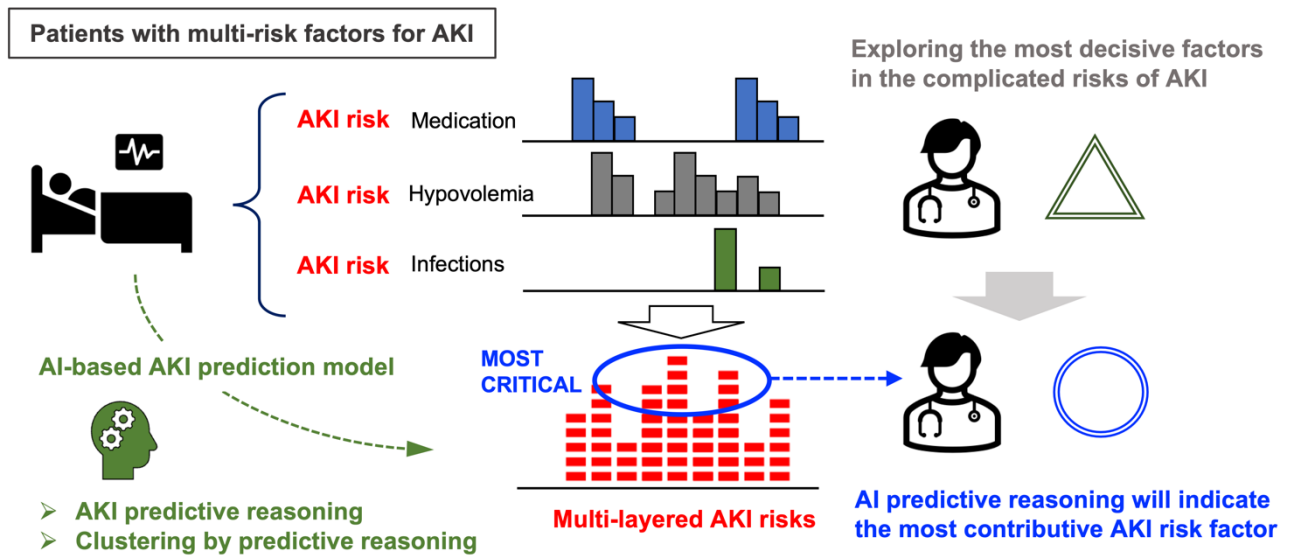
S3 Fig. Visualizing individual AKI predictive reasoning and clustering

ML-based unsupervised hierarchical clustering of 112 patients with AKI by SHAP values was performed. The clinical validity of the clustering was evaluated by comparing the predictive reasoning with the assessment of the nephrologists. AKI, acute kidney injury; ML, machine learning; SHAP, SHapley Additive exPlanations; SCr, serum creatinine.



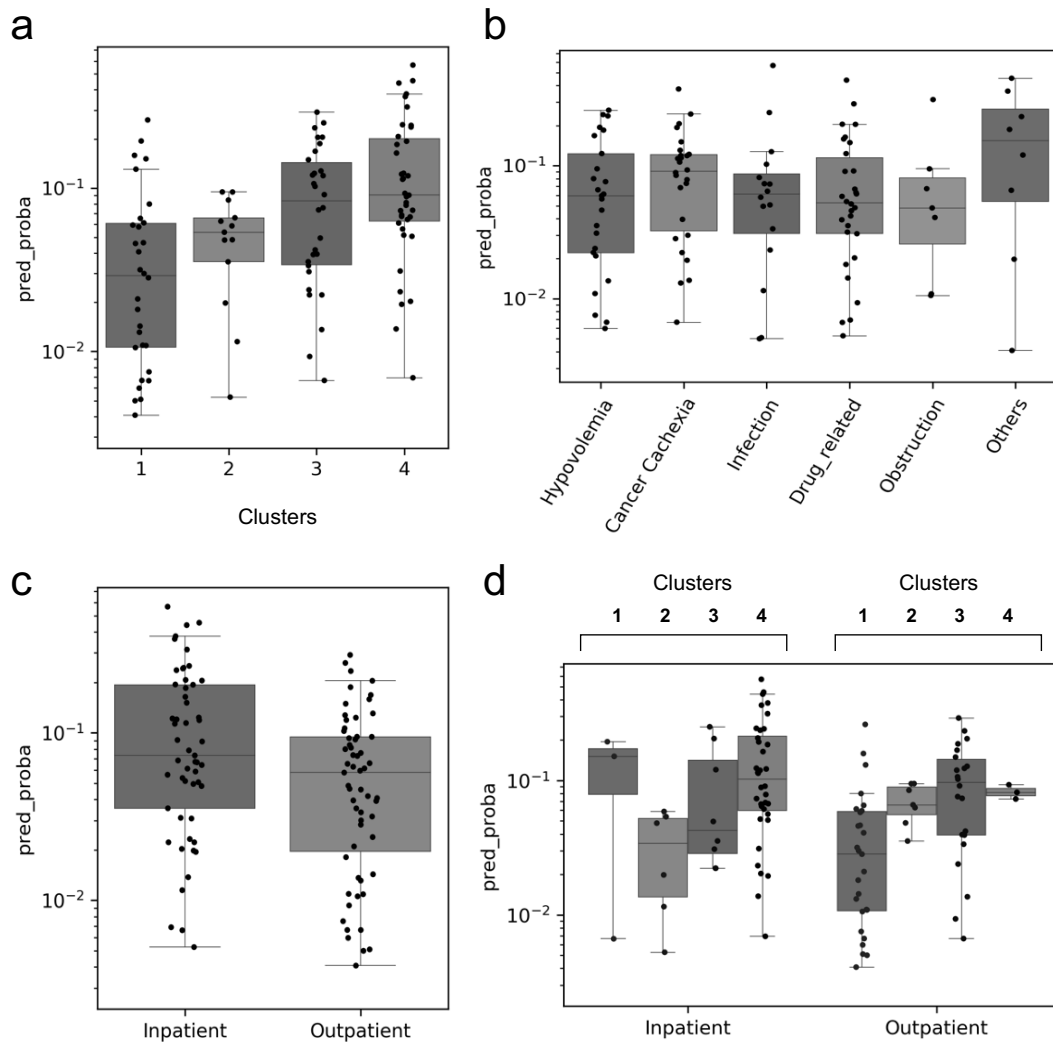
S4 Fig. Dependence plot of key features among 112 patients with AKI

Each point represents the correlation between the key feature values and their SHAP values in the week prior to each AKI development among these patients. AKI, acute kidney injury; SHAP, SHapley Additive exPlanations.



S5 Fig. Example of the future application of individual predictive reasoning

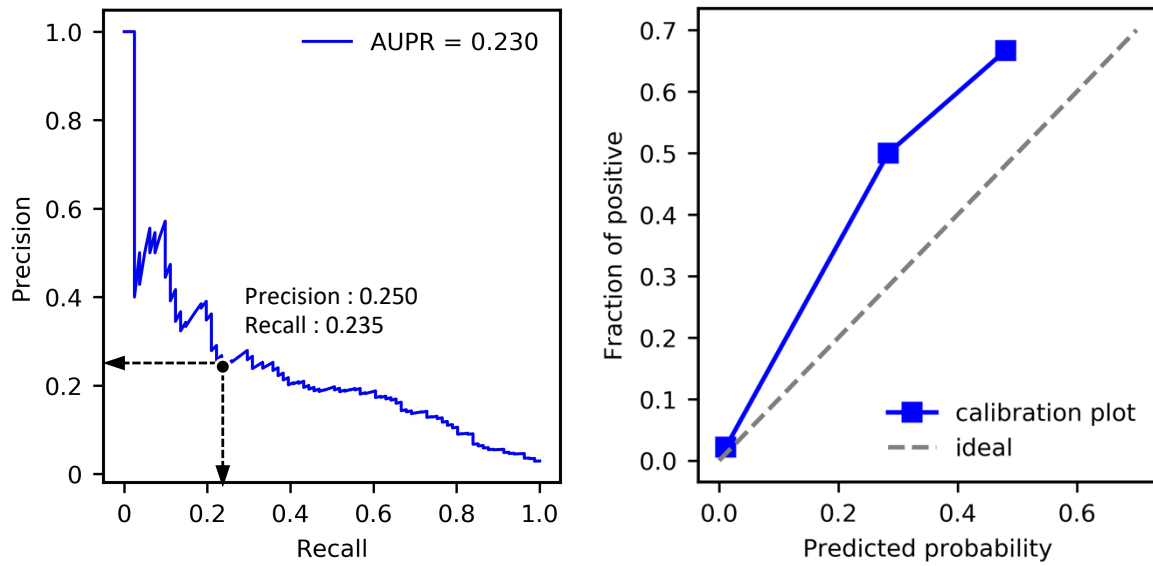
The application of individual predictive reasoning of AI models can be a valuable approach in exploring the most critical AKI risk from complicated AKI risks, which may be challenging to understand from routine medical information. AKI, acute kidney injury; AI, artificial intelligence.



S6 Fig. Prediction Probabilities in each cluster

(a) Prediction probabilities in each cluster. Cluster 4 has the highest prediction probability, while cluster 1 has the lowest prediction probability. (b) Prediction probability of a factor of AKI development annotated by the nephrologists, with no significant difference in prediction probability among the six labels. (c) Prediction probabilities for inpatients and outpatients with AKI. Prediction probabilities are higher for inpatients than for outpatients. (d) The proportion of inpatients and outpatients with AKI in each cluster.

Cluster 4 has more inpatients with AKI, whereas clusters 1 and 3 have more outpatients with AKI. These results suggest that the difference in predictive probability between clusters is more likely influenced by whether patients are in- or outpatients rather than by differences in causal factors for developing AKI. AKI, acute kidney injury.



S7 Fig. Precision-Recall curve and calibration plot

The Precision-Recall curve of the prediction model is presented; the positive prediction was determined using a threshold (red dotted line in Figure 2d) at which the precision is 0.25, as reported by Tomašev et al.^{S2}

S1 Table. Comparative performance of various machine learning models

	LR	SVM *	CatBoost	XGBoost	LightGBM
AUROC (mean)	0.702	0.526	0.837	0.851	0.880
Run time (mean \pmSD)	1.45s \pm 0.052s	40.4s \pm 25.4s	32.1s \pm 0.375s	5.12s \pm 0.086s	1.24s \pm 0.038s

Performance comparisons were conducted using different machine learning models on the same dataset. The models that were evaluated included Logistic Regression (LR), Support Vector Machine (SVM), CatBoost, XGBoost, and LightGBM. Each model was executed ten times to calculate the average values of the Area Under the Receiver Operating Characteristic (AUROC) and computational time. Due to the extensive computation time required by SVM, the analysis for this model was performed on a 10% sampled subset of the actual dataset (*). LR and SVM required preprocessing to address the missing values either through interpolation or deletion. Among the evaluated models, LightGBM exhibited the highest accuracy and demonstrated the capability for high-speed computation. The performance evaluations were carried out on a system equipped with two Intel(R) Xeon(R) Silver 4114 CPUs (2.20GHz, x86_64 architecture). The versions of the Python libraries used for the comparison were CatBoost version 1.2.2 (<https://catboost.ai/en/docs/>), XGBoost version 1.6.2 (<https://xgboost.readthedocs.io/en/stable/#>), scikit-learn 0.22.1 (<https://scikit-learn.org/stable/index.html>), and LightGBM 2.3.0 (<https://lightgbm.readthedocs.io/en/stable/#>).

S2 Table. Details of “Drug-related AKI Causes” by annotation in Clusters 2 and 3

	Annotation by nephrologists	ICI involvement	Days from ICI	Other risks for AKI	Renal biopsy
			initiation	development	
Cluster 2 (n = 6)	<i>AKI due to anorexia and dehydration caused by digestive IrAE</i>	Digestive IrAE	358 days	Dehydration Poor dietary intake	None
	<i>AKI associated with the worsening of general condition due to IrAE</i>	Systemic IrAE	31 days	Poor dietary intake	None
	<i>AKI due to renal IrAE with nephrosis and dehydration with fever</i>	ICI-AKI s/o	215 days	Dehydration	None
	<i>AKI associated with the worsening of general condition due to IrAE</i>	Systemic IrAE	104 days	Chronic kidney disease	None
	<i>Drug-induced AKI due to ICI and NSAIDs</i>	ICI-AKI s/o	109 days	NSAIDs	None
	<i>AKI associated with the worsening of general condition due to IrAE with fever and thrombocytopenia</i>	Systemic IrAE with thrombocytopenia	4 days	Poor dietary intake	None
	<i>AKI due to drug-induced kidney injury from levofloxacin and NSAIDs</i>	—	451 days	—	None
	<i>AKI associated with fever, colitis, and pneumonia due to IrAE</i>	Digestive and systemic IrAE	75 days	Pneumonia	None

Cluster 3 (n = 10)	<i>AKI due to drug-induced interstitial nephritis with garenoxacin</i>	—	22 days	—	None
	<i>AKI due to worsening of general condition from IrAE with alveolar hemorrhage and drug-induced renal injury from vancomycin</i>	Systemic IrAE with alveolar hemorrhage	101 days	Vancomycin In the intensive care unit	None
	<i>AKI due to drug-induced kidney injury from paclitaxel</i>	—	890 days	—	None
	<i>AKI due to worsening of general condition from systemic IrAE with drug eruption and renal IrAE</i>	Systemic IrAE with drug eruption and ICI-AKI s/o	15 days	Poor dietary intake	None
	<i>ICI-associated AKI due to nivolumab and kidney injury from NSAIDs</i>	ICI-AKI s/o	14 days	NSAIDs	Interstitial nephritis
	<i>AKI due to renal IrAE with proteinuria</i>	ICI-AKI s/o	20 days	—	None
	<i>AKI due to poor dietary intake and dehydration caused by systemic IrAE</i>	Systemic IrAE	155 days	Poor dietary intake Dehydration	None
	<i>AKI due to dehydration and poor dietary intake due to diarrhea in digestive IrAE</i>	Digestive IrAE	16 days	Poor dietary intake Dehydration	None

The annotations by nephrologists on factors contributing to AKI development and other AKI risk factors in cluster 2

(n = 6) and cluster 3 (n = 10), where “AKI due to drug involvement” was the most dominant factor. The gray areas

indicate cases where nephrologists determined that AKI development was related to ICI or IrAE. Among the cases labeled as “AKI due to drug involvement,” ICI was directly or indirectly involved in AKI development in 6 (100%) and 7 (70%) cases in cluster 2 and cluster 3, respectively.

AKI, acute kidney injury; ICI, immune checkpoint inhibitors; IrAE, immune-related adverse events; ICI-AKI s/o, suspicion of immune checkpoint inhibitors-associated acute kidney injury; NSAIDs, nonsteroidal anti-inflammatory drugs.

S3 Table. Details of “Other AKI Causes” by annotation

Details of factors contributing to AKI development	
Cluster 1 (n = 2)	Rhabdomyolysis (n =1), Cardiopulmonary arrest (n =1)
Cluster 2 (n = 1)	Hypercalcemia (n = 1)
Cluster 3 (n = 3)	Thrombotic microangiopathy (n = 1), Cardiopulmonary arrest (n = 1), Post-renal resection (n = 1)
Cluster 4 (n = 2)	Cardiopulmonary arrest (n = 1), Shock due to gastrointestinal perforation (n = 1)

Details of cases labeled “AKI due to other factors” by nephrologists in each cluster.

AKI, acute kidney injury.

Supporting References

S1. Kellum JA, Lameire N, Aspelin P, Barsoum RS, Burdmann EA, Goldstein SL, et al. Kidney disease: Improving global outcomes (KDIGO) acute kidney injury workgroup. KDIGO clinical practice guideline for acute kidney injury. *Kidney Int Suppl.* 2012;2: 1–138.

S2. Tomašev N, Glorot X, Rae JW, Zielinski M, Askham H, Saraiva A, et al. A clinically applicable approach to continuous prediction of future acute kidney injury. *Nature.* 2019;572:116–119. doi: 10.1038/s41586-019-1390-1.